J. Fluid Mech. (1970), *vol.* 43, *part* 2, *pp.* 225–246
Printed in Great Britain

Motion produced by combination of gravity and pressure differential when a gate in a tank of liquid is broken

By W. S. CHIU, M. Y. JAFFRIN AND A.H. SHAPIRO
Fluid Mechanics Laboratory, Department of Mechanical Engineering,
Massachusetts Institute of Technology

(Received 28 December 1969)

A two-dimensional, semi-infinite tank, closed by a vertical wall at one end, is initially filled to a certain level with an inviscid liquid at rest. A gate in the lower part of the wall is suddenly opened to a region where the gas pressure is greater or less than the gas pressure over the free liquid surface in the tank. The liquid escapes (or moves inwardly) through the gate under the combined action of gravity and the driving pressure differential. The fluid motion, the shapes of the two free surfaces, and the discharge through the gate are calculated for small times after the opening.

1. Introduction

The unsteady motions that occur when a dam suddenly disintegrates, and the water in an open reservoir behind the dam escapes, have been calculated for the two-dimensional case by Pohle (1952), and the results reported by Stoker (1957). This problem contains the difficulty of a free-surface boundary condition, and the analytical solution is known for small times only.

In this paper, a more general problem is treated (see figure 1), which differs in two ways from that of Pohle. First, the reservoir is replaced by a closed tank, such that the pressure over the free surface of the liquid in the tank is either greater, or smaller, than the pressure in the space to which the gate communicates; accordingly, the liquid motions are produced by a combination of gravity and of the pressure differential. Secondly, the entire end wall does not disappear; instead, at the bottom of the end wall, a gate (whose height is less than that of the liquid) is suddenly opened.

One application of this problem is to the rapid opening or bursting of a gate, valve, or pressure-relief disk in a gas-pressurized container of liquid.

Another application is to the inflation of a limp gas-filled balloon placed in the human aorta. The intra-aortic balloon pump is one of the more promising methods of temporary left-ventricle assistance for patients in heart failure (see Kolff, Moulopoulos & Topaz 1962; McMahon 1969). Since the balloon wall is limp, and the gas density inside the balloon is much less than that of the blood surrounding the balloon, the outer surface of the balloon is at uniform pressure.

This free-surface boundary condition makes the balloon problem somewhat like that treated in this paper. In the gate-opening problem, the free surface falls most rapidly adjacent to the end wall of the tank. Correspondingly, when an intra-aortic balloon is inflated by applying an excess gas pressure within the balloon, the inflation occurs first at the ends of the balloon in so-called 'bubbles'. This mode of balloon inflation, which can be modelled at least roughly by the gate-opening problem, is undesirable, because it can produce occlusion of the aorta and high pressures between the occlusive bubbles, and also because it can limit the usable volume displacement of the balloon.

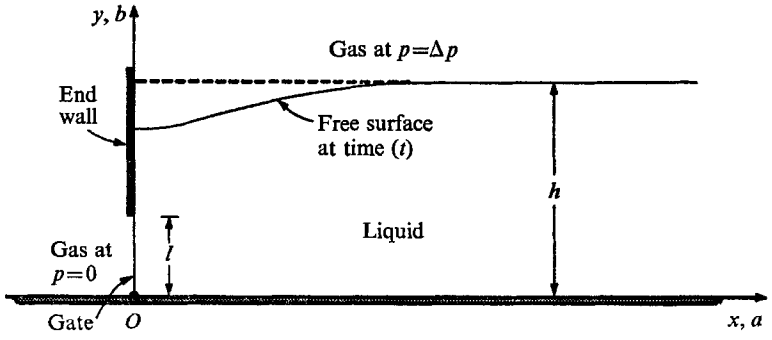

FIGURE 1. Geometry of the problem.

2. Formulation of the problem

Figure 1 shows a two-dimensional semi-infinite tank filled to the depth h with an inviscid liquid initially at rest. The gas pressure over the free surface of the liquid in the tank is constant and equal to Δp, which may be either positive or negative. At time $t = 0$, a gate of height l is suddenly opened at the end wall, allowing the liquid to escape into a space where the pressure is zero.

Our objectives are to determine the pressure distribution, the motion of the fluid, the shape and position of the free surfaces, and the flow discharged through the gate. As in Pohle's (1952) treatment, the problem is solved in closed form only for small values of the time t.

Two dimensionless parameters govern the problem: (i) l/h defines the geometry; and (ii) $\Delta p/\rho gh$ establishes the relative importance of the imposed pressure differential and of gravity in producing the motions. For the problem treated by Pohle (1952), these parameters have the particular values $l/h = 1$ and $\Delta p/\rho gh = 0$. We consider here the entire range

$$0 \leqslant l/h \leqslant 1 \quad \text{and} \quad -\infty \leqslant \Delta p/\rho gh \leqslant \infty.$$

(i) *Governing equations in Lagrangian co-ordinates*

Boundary conditions on free surfaces are expressed most simply in Lagrangian co-ordinates. The variables $x(a, b; t)$ and $y(a, b; t)$ denote the co-ordinates at time t of the fluid particle whose initial co-ordinates at the time $t = 0$ are a and b,

while $p(a,b;t)$ is the corresponding pressure. The equations of motion in Lagrangian variables are

$$x_{tt} = -p_x/\rho, \tag{1a}$$

$$y_{tt} = -p_y/\rho - g, \tag{1b}$$

where ρ is the density, g is the acceleration of gravity, and $p_x = \partial p/\partial x$, etc.

(ii) *Normalized variables*

It is convenient to introduce the following dimensionless variables:

$$X \equiv \pi x/2h, \qquad Y \equiv \pi y/2h,$$

$$A \equiv \pi a/2h, \qquad B \equiv \pi b/2h, \qquad D \equiv (\tfrac{1}{2}\pi)(l/h),$$

$$T \equiv t/(2h/\pi g)^{\frac{1}{2}}, \qquad P \equiv (\tfrac{1}{2}\pi)(p/\rho g h).$$

In the normalization of t, it is assumed that gravity is an important factor in the fluid motion and the corresponding time scale is therefore chosen as $(h/g)^{\frac{1}{2}}$. If $\Delta p/\rho g h \gg 1$, on the contrary, the motion is caused mainly by the pressure difference and a more appropriate choice of time scale would be $(\rho h^2/\Delta p)^{\frac{1}{2}}$; (2*a*) and (2*b*) (which follow) would then be different in form. Note, however, that the validity of the results does not depend upon which time scale is used.

Equations (1*a*) and (1*b*) now become

$$X_{TT} = -P_X, \tag{2a}$$

$$Y_{TT} = -P_Y - 1. \tag{2b}$$

On eliminating the partial derivatives with respect to X and Y in (2*a*) and (2*b*), we obtain the equations of motion in the form,

$$X_{TT}X_A + (Y_{TT}+1)Y_A + P_A = 0, \tag{3a}$$

$$X_{TT}X_B + (Y_{TT}+1)Y_B + P_B = 0. \tag{3b}$$

In the Lagrangian description, the two-dimensional equation of continuity of an incompressible fluid may be written by setting the Jacobian of the transformation $(X, Y) \rightarrow (A, B)$ equal to unity:

$$X_A Y_B - X_B Y_A = 1. \tag{4}$$

(iii) *Series expansion for small values of time*

By considering times much shorter than the characteristic time, namely for $T \ll 1$, a solution of the system of equations (3*a*), (3*b*) and (4) may be sought in the form of series expansions in T, which are here carried out to terms of order T^2:

$$X(A,B;T) = A + X^{(1)}(A,B)T + \tfrac{1}{2}X^{(2)}(A,B)T^2 + \ldots, \tag{5a}$$

$$Y(A,B;T) = B + Y^{(1)}(A,B)T + \tfrac{1}{2}Y^{(2)}(A,B)T^2 + \ldots, \tag{5b}$$

$$P(A,B;T) = P^{(0)}(A,B) + P^{(1)}(A,B)T + \tfrac{1}{2}P^{(2)}(A,B)T^2 + \ldots. \tag{5c}$$

In these expressions, $X^{(1)}$ and $Y^{(1)}$ are the dimensionless initial velocity components; $X^{(2)}$ and $Y^{(2)}$ are the dimensionless initial acceleration components; and $P^{(0)}(A,B)$ is the dimensionless initial pressure field.

(iv) *Initial conditions*

Equations (5a) and (5b) automatically satisfy the initial conditions of displacement at $T = 0$. Since the flow starts from rest, i.e.

$$X_T(A, B; 0) = Y_T(A, B; 0) = 0,$$

it follows that

$$X^{(1)} = Y^{(1)} = 0. \tag{6}$$

(v) *Governing equations for $X^{(2)}$ and $Y^{(2)}$*

Substituting (5a) and (5b) and (6) into (4), and equating the coefficients of T^2, we get

$$X_A^{(2)} + Y_B^{(2)} = 0. \tag{7}$$

The pressure may be eliminated from (3a) and (3b) by cross-differentiation. Then, by substituting the expansions (5a) and (5b) into the resulting equations, and considering the coefficients of T^2, we obtain

$$X_B^{(2)} - Y_A^{(2)} = 0. \tag{8}$$

For terms up to T^2, the motion is governed by (7) and (8), which are, respectively, the equation of continuity and the equation of irrotationality.

(vi) *Boundary conditions*

For small times at least, fluid particles on the two free surfaces can be assumed to remain on the free surface. Defining $\Delta P \equiv (\frac{1}{2}\pi)(\Delta p/\rho g h)$, therefore, we set

$$P(A, \tfrac{1}{2}\pi; T) = \Delta P, \quad \text{for} \quad 0 \leqslant A \leqslant \infty. \tag{9}$$

In considering the boundary condition for the free surface formed at the gate, we face the difficulty that this boundary is formed not only of particles originally at the gate, but also of some particles originally on the wall, at $A = 0, D \leqslant B \leqslant \frac{1}{2}\pi$, which move out through the gate and become part of the free boundary. However, since we restrict the solution to $T \ll 1$, the particles do not move very far. Thus, we may approximate the true free-surface boundary condition by applying it only to those particles originally in the free surface:

$$P(0, B; T) = 0, \quad \text{for} \quad 0 \leqslant B \leqslant D. \tag{10}$$

A similar consideration applies to the boundary condition for particles originally at the wall, i.e. $A = 0$, $D \leqslant B \leqslant \frac{1}{2}\pi$. Some of these particles, as mentioned above, escape through the gate, and thus do not remain at the wall. But, again making an approximation consistent with $T \ll 1$, we assume that the particles originally at the wall remain at the wall. The approximate boundary condition is thus

$$X(0, B; T) = 0, \quad \text{for} \quad D \leqslant B \leqslant \tfrac{1}{2}\pi. \tag{11}$$

For particles originally on the bottom, the boundary condition is

$$Y(A, 0; T) = 0, \quad \text{for} \quad 0 \leqslant A < \infty. \tag{12}$$

At any finite time, the fluid infinitely far from the wall is at rest; hence,

$$X_T(\infty, B; T) = Y_T(\infty, B; T) = 0, \quad \text{for} \quad 0 \leqslant B \leqslant \tfrac{1}{2}\pi. \tag{13}$$

(vii) *Boundary conditions for* $X^{(2)}$ *and* $Y^{(2)}$

The corresponding boundary conditions for $X^{(2)}$ and $Y^{(2)}$ can be obtained by substituting (5(a), (b) and (c)) into the boundary conditions above. Equations (11) and (12) give, respectively,

$$X^{(2)}(0, B) = 0, \quad \text{for} \quad 0 \leqslant B \leqslant \tfrac{1}{2}\pi, \tag{14}$$

$$Y^{(2)}(A, 0) = 0, \quad \text{for} \quad 0 \leqslant A \leqslant \infty. \tag{15}$$

The substitution of (5) into (3a) yields, to the lowest order,

$$P_A^{(0)} = -X^{(2)}(A, B). \tag{16}$$

The term $P_A^{(1)}$ is zero, while the term $P_A^{(2)}$ contributes only terms in T^2 and higher, which, compared with $P_A^{(0)}$, can be neglected in what follows, since $T \ll 1$. Keeping this in mind, differentiating (9) with respect to A, and using equation (16), we obtain

$$X^{(2)}(A, \tfrac{1}{2}\pi) = 0 \quad \text{for} \quad 0 \leqslant A < \infty. \tag{17}$$

A similar procedure applied to (3b) and (10a) gives

$$P_B^{(0)} = -Y^{(2)}(A, B) - 1, \tag{18}$$

and

$$Y^{(2)}(0, B) = -1 \quad \text{for} \quad 0 \leqslant B \leqslant D. \tag{19}$$

From (13),

$$X^{(2)}(\infty, B) = Y^{(2)}(\infty, B) = 0 \quad \text{for} \quad 0 \leqslant B \leqslant \tfrac{1}{2}\pi. \tag{20}$$

It is essential to note that the pressure difference Δp has been eliminated from the boundary conditions by differentiation. Accordingly, the solutions for $X^{(2)}$ and $Y^{(2)}$, satisfying the boundary conditions of (14), (15), (17), (19) and (20), will not be unique, but will contain an unknown parameter. This parameter is determined by reintroducing the condition that the pressure difference between the free surface and the chamber downstream of the gate is equal to Δp. In dimensionless form,

$$\Delta P = \int_{\mathrm{I}}^{\mathrm{II}} \nabla P \cdot d\mathbf{r}, \tag{21}$$

where I and II are any locations having the following co-ordinates:

$$\mathrm{I}: A = 0 \quad \text{along} \quad 0 < B < D,$$

$$\mathrm{II}: B = \tfrac{1}{2}\pi \quad \text{along} \quad A > 0,$$

and $d\mathbf{r}$ is the unit vector along any curve connecting I and II.

3. Method of solution

The variables $X^{(2)}$ and $-Y^{(2)}$ are conjugate functions satisfying the Cauchy–Riemann relations according to (7) and (8). Therefore, the solution to these equations is most readily found by introducing the complex quantities $Z = A + iB$, representing the physical plane; and $W(Z) = X^{(2)}(A, B) - iY^{(2)}(A, B)$. By virtue of (7) and (8), $W(Z)$ is an analytic function.

Figure 2 shows the boundary conditions in the Z-plane as determined by equations (14), (15), (17), (19) and (20), together with (7) and (8). Neither $X^{(2)}$ nor $Y^{(2)}$ is known over the entire boundary of the domain. The problem is of Cauchy type, since on some segments a directional derivative of $Y^{(2)}$ is prescribed, while on the others $Y^{(2)}$ itself is prescribed. It is desirable to convert the boundary-value problem to one of Dirichlet type, with one of the two dependent variables (we choose $Y^{(2)}$) prescribed over the entire boundary. This may be done by means of analytic continuations and conformal mappings. The co-ordinates of corresponding points in the different complex planes are listed in table 1.

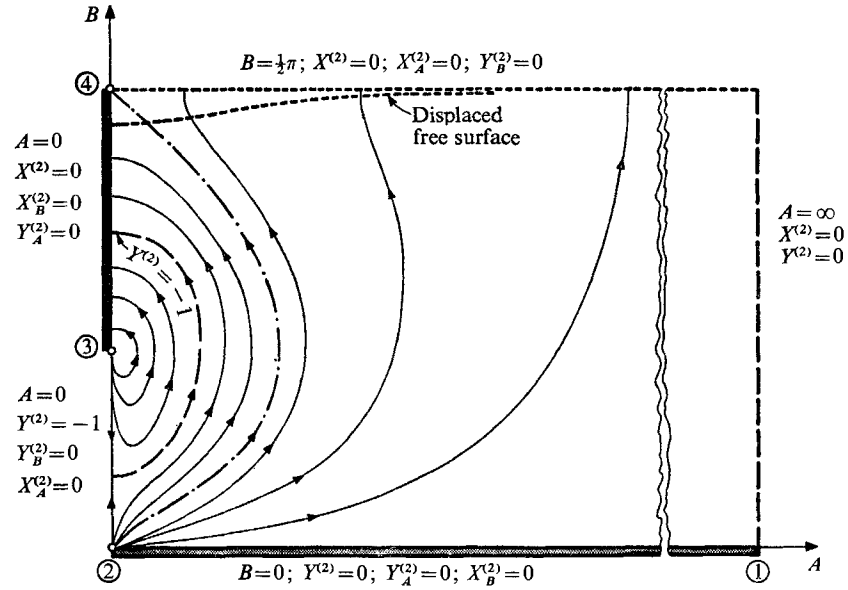

FIGURE 2. The complex plane $Z = A + iB$, showing the boundary conditions. The contours of constant $Y^{(2)}$ are for values of ΔP such that $\mu > 0$ but is not large (see caption for figure 12).

Point	Z	$\zeta_1 = \cosh^{-1}\left(\frac{\cosh Z}{\cos D}\right)$	$\zeta_2 = \exp\zeta_1$ (see footnote)
1	$+\infty$	$+\infty$	∞
2	0	$\cosh^{-1}(1/\cos D)$	
3, 3′	iD	0	1
2′		$-\cosh^{-1}(1/\cos D)$	λ^{-1}
1′		$-\infty$	0
7′		$-\infty+i\pi$	0
6′		$-\cosh^{-1}(1/\cos D)+i\pi$	$-\lambda^{-1}$
5′, 5	$i(\pi-D)$	$i\pi$	-1
6	$i\pi$	$\cosh^{-1}(1/\cos D)+i\pi$	$-\lambda$
7	$\infty+i\pi$	$\infty+i\pi$	$-\infty$
4, 4′	$i\pi/2$	$i\pi/2$	i

TABLE 1.†

† $\lambda \equiv \exp[\cosh^{-1}(1/\cos D)]$.

(i) *Reflexion about the line* $B = \frac{1}{2}\pi$

On differentiating equation (17) and using the Cauchy–Riemann relations, one obtains

$$Y^{(2)}_B(A, \tfrac{1}{2}\pi) = 0 \quad \text{for} \quad 0 \leqslant A < \infty.$$

Thus, the solution for $Y^{(2)}$ can be continued analytically beyond the line $B = \frac{1}{2}\pi$ by reflexion and a semi-infinite half-strip of height π can be constructed. The additional boundary conditions shown in figure 3 are determined by symmetry considerations.

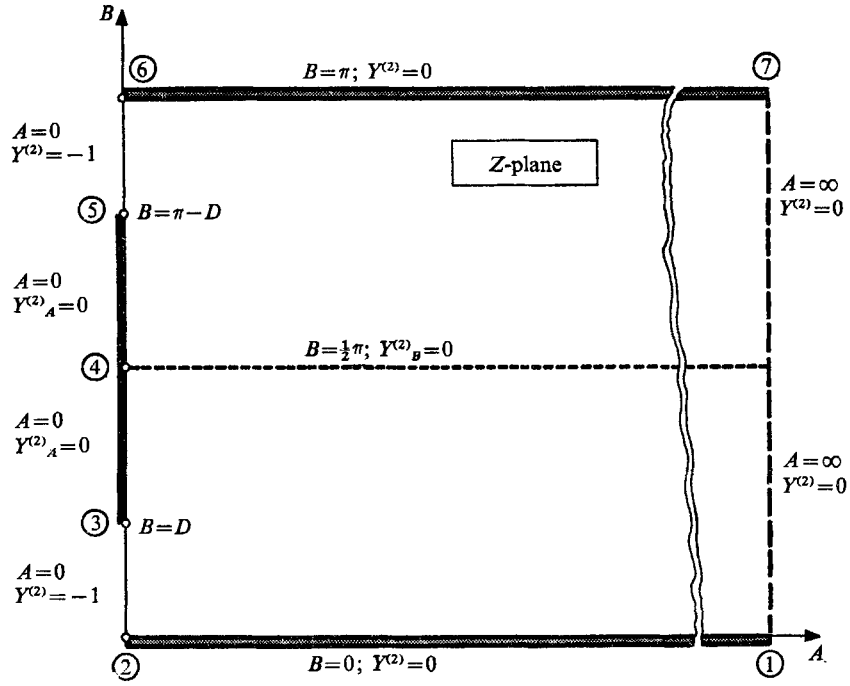

FIGURE 3. The Z-plane, showing analytic continuation across $B = \frac{1}{2}\pi$ by reflexion, and the corresponding boundary conditions.

(ii) *Mapping from Z-plane to* ζ_1*-plane*

The Schwartz–Christoffel transformation,

$$\zeta_1 = \cosh^{-1}(\cosh Z/\cos D), \tag{22}$$

now maps the points $(0, D)$ and $(0, \pi - D)$ of the Z-plane into the points $(0, 0)$ and $(0, \pi)$, respectively, of the ζ_1-plane. The new domain and the corresponding boundary conditions are shown on the right half of figure 4.

(iii) *Reflexion about* $\xi_1 = 0$

On the boundary segments 3–4 and 4–5, the boundary condition is $Y^{(2)}_A = 0$. In the transformed co-ordinates, this becomes

$$Y^{(2)}_{\xi_1} = 0, \quad \text{for} \quad \xi_1 = 0.$$

This condition permits the solution for $Y^{(2)}$ in the right half-strip of figure 4 to be analytically continued, by reflexion across ξ_1 the axis = 0, into the left half-strip. The boundary conditions on the left half-strip are determined by considerations of symmetry. It is seen that the function $Y^{(2)}$ is now prescribed over the entire boundary of an infinite strip.

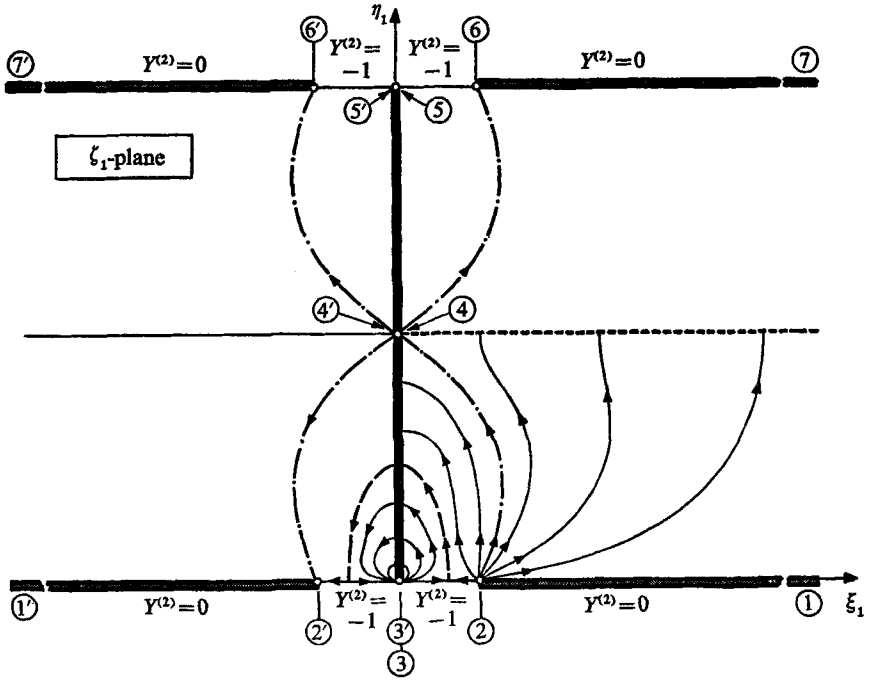

FIGURE 4. The ζ_1-plane, showing the boundary conditions for $Y^{(2)}$, analytical continuation across $\xi_1 = 0$ by reflexion, and contours of constant $Y^{(2)}$.

(iv) *Mapping to the half-plane* ζ_2

The final step is to map the infinite strip of figure 4 into the upper half-plane of figure 5 by means of the tranformation,

$$\zeta_2 = \exp[\zeta_1] = \exp[\cosh^{-1}(\cosh Z/\cos D)]. \tag{23}$$

The straight line 3–4–5 in the ζ_1-plane maps into the semicircle of unit radius in the ζ_2-plane. The right half-strip of the ζ_1-plane maps into the region outside the semicircle in the ζ_2-plane, while the left half-strip maps into the region inside the semicircle. The physical Z-plane (figure 2) is mapped onto the space to the right of and above the contour 1–2–3–4 of the ζ_2-plane. Figure 5 shows the appropriate boundary conditions for $Y^{(2)}$ in the ζ_2-plane.

(v) *The solution function* $W(\zeta_2)$

To determine the formation of the function $W(\zeta_2)$ whose imaginary part $-Y^{(2)}$ satisfies the boundary conditions shown on figure 5, we now introduce singularities that are consistent with these boundary conditions. That discontinuities in the boundary conditions exist at points 2, 3, 5, 6 in the Z-plane requires that there be singularities at those points. Corresponding singularities occur at points 2, 3,

5 and 6 of the ζ_1-plane and of the ζ_2-plane, as well as at their reflexions 2′, 3′, 5′ and 6′. Special care must be taken on the line segments 2–3–3′–2′ and 6–5–5′–6′. In order to be able to satisfy (21), one must admit the possibility of singularities at 3, 3′, and 5 and 5′ even though the values of $Y^{(2)}$ on these two lines are continuous in the ζ_2-plane.

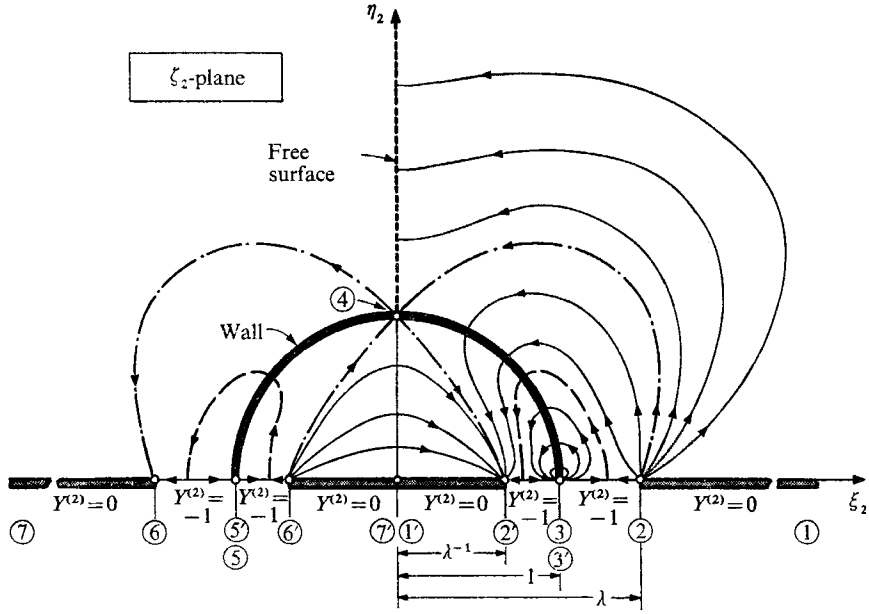

FIGURE 5. The ζ_2-plane, showing the boundary conditions for $Y^{(2)}$. The contours of constant $Y^{(2)}$ have arrows which indicate the direction of flow if points 2 and 6′ are thought of as physical sources, 2′ and 6 as physical sinks, and 3 and 5 as physical doublets.

The appropriate singularities are two sinks of strength 2 located at $\zeta_2 = +\lambda^{-1}$, $-\lambda$, two sources of strength 2 located at $\zeta_2 = +\lambda$, $-\lambda^{-1}$, and two doublets of as yet unknown strength located at $\zeta_2 = \pm 1$, where

$$\lambda = \exp[\cosh^{-1}(1/\cos D)].$$

The complex potential $W(\zeta_2)$ may now be immediately written down as

$$W(\zeta_2) = \frac{1}{\pi}\ln\frac{(\zeta_2-\lambda)(\zeta_2+\lambda^{-1})}{(\zeta_2+\lambda)(\zeta_2-\lambda^{-1})} - 2\mu\left(\frac{1}{\zeta_2-1}+\frac{1}{\zeta_2+1}\right). \tag{24}$$

The quantity μ for the doublets will be determined later by means of (21).

(vi) *The solution function* $W(Z)$

By using the inverse transformation $\zeta_2 \to Z$, as given by (23), (24) is brought into the form,

$$W(Z) = X^{(2)} - iY^{(2)} = (1/\pi)[\ln(\tanh Q) - \ln(\tanh R)] - 2\mu/\sinh[\cosh^{-1}(\cosh Z/\cos D)], \tag{25}$$

where

$$Q = \tfrac{1}{2}[\cosh^{-1}(\cosh Z/\cos D) - \cosh^{-1}(1/\cos D)],$$

$$R = \tfrac{1}{2}[\cosh^{-1}(\cosh Z/\cos D) + \cosh^{-1}(1/\cos D)].$$

Then, substituting $Z = A + iB$ into (25), and separating the real and imaginary parts, we get

$$X^{(2)} \equiv \alpha_1 + \mu\alpha_2, \tag{26a}$$

$$Y^{(2)} \equiv \beta_1 + \mu\beta_2, \tag{26b}$$

where

$$\alpha_1 = \frac{1}{2\pi} \ln[(R_1^2 + R_2^2)/(Q_1^2 + Q_2^2)], \tag{27a}$$

$$\alpha_2 = -\frac{2\Omega^2(\Omega^2-1)^{\frac{1}{2}} \cos D \cosh A \cos B}{\Omega^4 \cos^2 D - \cosh^2 A \cos^2 B}, \tag{27b}$$

$$\beta_1 = \frac{1}{\pi} \tan^{-1}[(R_2 Q_1 - R_1 Q_2)/(R_1 Q_1 + R_2 Q_2)], \tag{27c}$$

$$\beta_2 = -\frac{2\Omega^2 \cos D(\Omega^2 \cos^2 D - \cosh^2 A \cos^2 B)^{\frac{1}{2}}}{\Omega^4 \cos^2 D - \cosh^2 A \cos^2 B}, \tag{27d}$$

$$\Omega = \frac{1}{2}\left\{\left[\left(1 + \frac{\cosh A \cos B}{\cos D}\right)^2 + \left(\frac{\sinh A \sin B}{\cos D}\right)^2\right]^{\frac{1}{2}} + \left[\left(1 - \frac{\cosh A \cos B}{\cos D}\right)^2 + \left(\frac{\sinh A \sin B}{\cos D}\right)^2\right]^{\frac{1}{2}}\right\}, \tag{27e}$$

$$Q_1 = \frac{(\Omega^2-1)^{\frac{1}{2}} - \Omega \sin D}{\Omega - (\Omega^2-1)^{\frac{1}{2}} \sin D - \Omega^{-1} \cosh A \cos B}, \tag{27f}$$

$$Q_2 = \frac{|\cos^2 D - (\Omega^{-1} \cosh A \cos B)^2|^{\frac{1}{2}}}{\Omega - (\Omega^2-1)^{\frac{1}{2}} \sin D - \Omega^{-1} \cosh A \cos B}, \tag{27g}$$

$$R_1 = \frac{(\Omega^2-1)^{\frac{1}{2}} + \Omega \sin D}{\Omega + (\Omega^2-1)^{\frac{1}{2}} \sin D - \Omega^{-1} \cosh A \cos B}, \tag{27h}$$

$$R_2 = \frac{|\cos^2 D - (\Omega^{-1} \cosh A \cos B)^2|^{\frac{1}{2}}}{\Omega + (\Omega^2-1)^{\frac{1}{2}} \sin D - \Omega^{-1} \cosh A \cos B}. \tag{27i}$$

It may be shown by substitution that the solutions for $X^{(2)}$ and $Y^{(2)}$ given by (26) and (27) do indeed satisfy the boundary conditions of (14), (15), (17), (19) and (20).

(vii) *Determination of* μ

It now remains to determine the value of μ from (21), using (16), (18), (26) and (27). Since the integral of (21) may be taken along any curve connecting any pair of points I and II on the two free surfaces, we choose for simplicity the segment on the end wall ($A = 0$) between $B = D$ and $B = \frac{1}{2}\pi$. The result of this calculation is

$$\Delta P = \mathscr{D}_1(D) + \mu\mathscr{D}_2(D), \tag{28}$$

where

$$\mathscr{D}_1(D) = -\int_D^{\frac{1}{2}\pi} [\beta_1(0, B) + 1]\, dB, \tag{29}$$

$$\mathscr{D}_2(D) = -\int_D^{\frac{1}{2}\pi} \beta_2(0, B)\, dB = 2\int_D^{\frac{1}{2}\pi} [1 - (\cos B/\cos D)^2]^{-\frac{1}{2}}\, dB, \tag{30}$$

for which the last part of (30) has been obtained using (26) and (27). With the transformation $\sin\psi = \cos B/\cos D$, (30) becomes

$$\mathscr{D}_2(D) = 2\cos D\int_D^{\frac{1}{2}\pi}(1-\cos^2 D\sin^2\psi)^{-\frac{1}{2}}\,d\psi$$
$$= 2(\cos D)\cdot K(\cos D), \tag{31}$$

where $K(\cos D)$ denotes the complete elliptic integral of the first kind, with the argument $\cos D$.

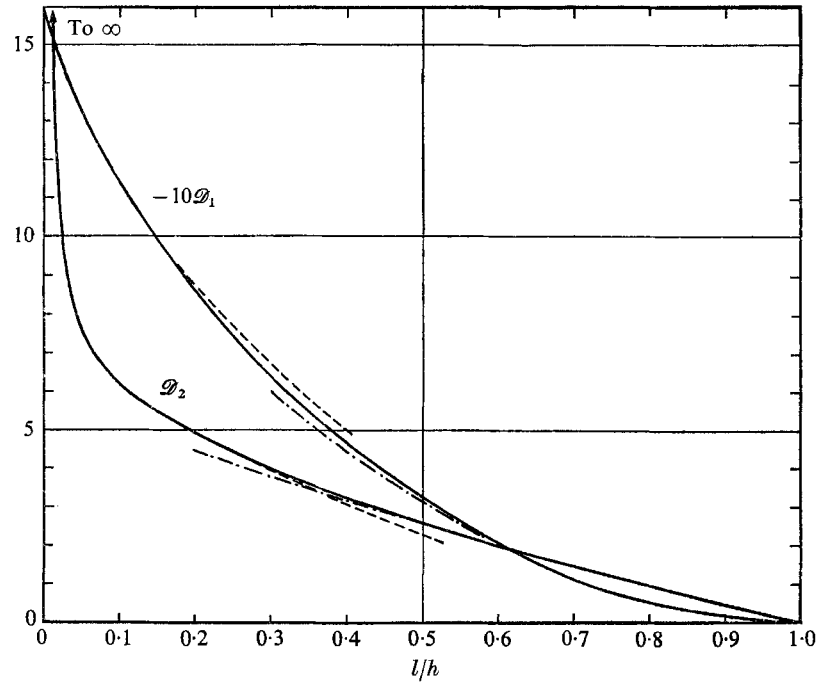

FIGURE 6. The functions $\mathscr{D}_1(D)$ and $\mathscr{D}_2(D)$: ——, exact solution, (29) and (31); – – –, expansion solution, (45), for $l/h \ll 1$; —·—·—, expansion solution, (51), for $(1-l/h) \ll 1$.

The function $\mathscr{D}_1(D)$ is determined from (29) with equations (26) and (27) by means of numerical integration. The function $\mathscr{D}_2(D)$, according to (31), is obtained from tables of elliptic integrals. Table 2 lists numerical values of $\mathscr{D}_1(l/h)$, while figure 6 gives $\mathscr{D}_1$ and $\mathscr{D}_2$ graphically as functions of l/h. With these and (28), one may compute the doublet strength for arbitrary values of ΔP and D:

$$\mu(\Delta P, D) = (1/\mathscr{D}_2)(\Delta P - \mathscr{D}_1). \tag{32}$$

We see that μ is a linear function of ΔP.

(viii) *The functions* Γ *and* Π

The solutions for $X^{(2)}$ and $Y^{(2)}$ are now completely determined. Examination of (26) and (32) shows that $X^{(2)}$ and $Y^{(2)}$ may be brought into the forms

$$X^{(2)} = -\Gamma_X(A,B,D) - (\Delta p/\rho g h)\cdot\Pi_X(A,B,D), \tag{33a}$$
$$Y^{(2)} = -\Gamma_Y(A,B,D) - (\Delta p/\rho g h)\cdot\Pi_Y(A,B,D). \tag{33b}$$

The functions Γ_X, Γ_Y represent the influence of gravity, while Π_X, Π_Y represent the influence of the driving pressure difference Δp. That the motions at small time due, respectively, to gravity and to the pressure differential are linearly additive follows of course from the linearity of the governing equations (7) and (8) and of the boundary conditions, including (21). We observe, however, that the additive property of the pressure-induced and gravity-induced motions is not generally valid: it comes about in the present case, first, because the fluid is assumed initially at rest, and, second, because we consider terms in the displacement only up to order T^2.

l/h	0	0·1	0·2	0·3	0·4	
$-\mathscr{D}_1$	$\frac{1}{2}\pi$	1·1471	0·8668	0·6446	0·4639	
l/h	0·5	0·6	0·7	0·8	0·9	1·0
$-\mathscr{D}_1$	0·3203	0·2008	0·1121	0·0497	0·0124	0

TABLE 2

4. Results and discussion

We first note that the physical displacement, velocity, and acceleration components are respectively given by

$$\Delta x = (gt^2/2)X^{(2)}, \quad \Delta y = (gt^2/2)Y^{(2)}; \tag{34a}$$

$$x_t = gtX^{(2)}, \qquad y_t = gtY^{(2)}; \tag{34b}$$

$$x_{tt} = gX^{(2)} \qquad y_{tt} = gY^{(2)}. \tag{34c}$$

Thus, $X^{(2)}$ and $Y^{(2)}$ represent the physical displacements scaled to $gt^2/2$, the physical velocity components scaled to gt, and the physical acceleration components scaled to the acceleration of gravity.

(i) *Range of validity*

The solutions for the acceleration field, given by (26) and (27), and for the pressure field, given by (16) and (18), are exact only at $t = 0$, when the gate opens.

Because of the approximations used in the boundary conditions and of the necessity of rapid convergence of the series of (5), the solutions for the displacement and velocity components given by (33) and (34) are approximately correct only up to values of t for which the physical displacements are small compared with the physical dimensions of the problem.

If $\Delta P \gg 1$, so that the motion is dominated by the pressure differential, the same remarks apply. In that case, however, the magnitude of the time, up to which the displacements and velocities are good approximations, is determined by the condition that $T\sqrt{(\Delta P)} \ll 1$; rather than, as in the case of gravity-dominated motions, that $T \ll 1$.

When gravity is absent or negligible, $\Delta P \to \infty$. From (32), then, $\mu \cong \Delta P/\mathscr{D}_2$, and $\mu \to \infty$. Choosing $X^{(2)}$, for example, (26*a*) gives $X^{(2)} \cong \mu\alpha_2 \cong \alpha_2 \cdot \Delta P/\mathscr{D}_2$. The quantities $gX^{(2)}$ and $gY^{(2)}$ appearing in equations (34) may therefore be replaced by

$$gX^{(2)} = \frac{\pi}{2}\frac{\Delta p}{\rho h}\frac{\alpha_2}{\mathscr{D}_2}, \quad gY^{(2)} = \frac{\pi}{2}\frac{\Delta p}{\rho h}\frac{\beta_2}{\mathscr{D}_2}, \tag{35}$$

which are the convenient forms for $\Delta P \gg 1$.

(ii) *Values of $X^{(2)}$ and $Y^{(2)}$ at the boundaries*

A general picture of the displacement, velocity and acceleration fields may be gained from a presentation of the values of $X^{(2)}$ and $Y^{(2)}$ at the four boundaries. These are (1) the free surface (FS) above the liquid in the tank, where $b = h$, (2) the end wall (W), where $a = 0$, $l \leqslant b \leqslant h$, (3) the free surface at the gate opening (G) through which the liquid escapes, where $a = 0$, $0 \leqslant b \leqslant l$, and (4) the bottom (B) of the tank, where $b = 0$. In particular, the displacements of the two free surfaces are proportional to the values of $Y^{(2)}_{\mathrm{FS}}$ and $X^{(2)}_{\mathrm{G}}$.

In the formulas and graphs that follow, the respective contributions of gravity and of the pressure differential to $X^{(2)}$ and $Y^{(2)}$ are, according to (33), presented in terms of the appropriate functions Γ and Π at the four boundaries. For convenience, we employ in the graphs such quantities as a/h, b/h and l/h, rather than A, B, and D.

(*a*) *The free surface in the tank* (FS): $A \geqslant 0$, $B = \frac{1}{2}\pi$. Here $X^{(2)}_{\mathrm{FS}} = 0$, $\Gamma_{X,\mathrm{FS}} = 0$, and $\Pi_{X,\mathrm{FS}} = 0$, while

$$\Gamma_{Y,\mathrm{FS}} = \frac{2}{\pi}\tan^{-1}\left[\frac{\sin D}{(\cos^2 D + \sinh^2 A)^{\frac{1}{2}}}\right] - \frac{2\mathscr{D}_1}{\mathscr{D}_2(1+\sinh^2 A/\cos^2 D)^{\frac{1}{2}}}, \tag{36}$$

$$\Pi_{Y,\mathrm{FS}} = \pi/\mathscr{D}_2(1+\sinh^2 A/\cos^2 D)^{\frac{1}{2}}. \tag{37}$$

Figure 7 shows the functions $\Gamma_{Y,\mathrm{FS}}$ and $\Pi_{Y,\mathrm{FS}}$ plotted against a/h for several values of the gate-opening parameter l/h. The values of $\Gamma_{Y,\mathrm{FS}}$ are less than unity, indicating that gravity alone cannot produce at the free surface accelerations as large as gravity, except for the limiting case $l/h = 1$, where the surface accelerates downwards with the magnitude g at the point $a/h = 0$.

(*b*) *The end wall* (W): $A = 0$, $D \leqslant B \leqslant \frac{1}{2}\pi$. Here $X^{(2)}_{\mathrm{W}} = 0$, $\Gamma_{X,\mathrm{W}} = 0$ and $\Pi_{X,\mathrm{W}} = 0$. Since the fluid horizontal acceleration $X^{(2)}$ vanishes both on the end-wall and the free surface, it follows that $Y^{(2)} = iW(Z)$ is a function of Z on these boundaries. Therefore, the values of Γ_Y and Π_Y at the wall may be immediately deduced by substituting $Z = iB$ in place of $Z = A + i\pi/2$ in (36) and (37).

$$\Gamma_{Y,\mathrm{W}} = \frac{2}{\pi}\tan^{-1}\left[\frac{\tan D}{(1-\cos^2 B/\cos^2 D)^{\frac{1}{2}}}\right] - \frac{2\mathscr{D}_1}{\mathscr{D}_2(1-\cos^2 B/\cos^2 D)^{\frac{1}{2}}}, \tag{38a}$$

$$\Pi_{Y,\mathrm{W}} = \pi/\mathscr{D}_2(1-\cos^2 B/\cos^2 D)^{\frac{1}{2}}. \tag{38b}$$

Figure 8 shows these functions plotted against the abscissa $(b-l)/(h-l)$. Except for the limiting case $l/h = 1$ (which is singular and for which $\Gamma_{Y,\mathrm{W}} = 1$, $\Pi_{Y,\mathrm{W}} = \infty$), both sets of functions go to infinity at the lip of the gate where $b \to l$. This corresponds to the strong transformed-doublet singularity at $b = l$.

Because of this singularity, the value of $Y^{(2)}$ changes discontinuously from $-\infty$ to -1 at $b = l$.

Both sets of curves have zero slope at $b = h$, indicating that the vertical acceleration on the end wall is nearly constant over the region close to the free surface.

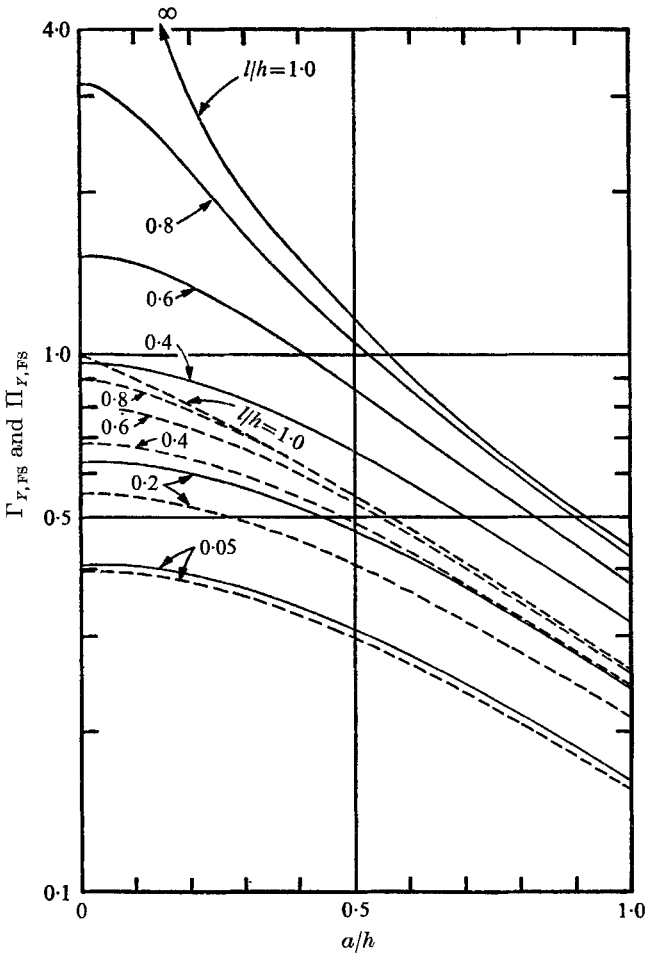

FIGURE 7. The functions Γ_Y and Π_Y for the free surface in the tank, as given by (36) and (37): ——, $\Pi_{Y,\mathrm{FS}}$; – – –, $\Gamma_{Y,\mathrm{FS}}$.

With gravity alone, the curves of $\Gamma_{Y,\mathrm{W}}$ cross unity at about $(b-l)/(h-l) \cong 0{\cdot}25$; hence, above the crossing point the downward vertical acceleration is less than g, below the crossing point it is greater than g.

(*c*) *The gate* (G): $A = 0$, $0 \leqslant B \leqslant D$. Here $Y^{(2)}_{\mathrm{G}} = -1$, $\Gamma_{Y,\mathrm{G}} = -1$, and $\Pi_{Y,\mathrm{G}} = 0$, while

$$\Gamma_{X,\mathrm{G}} = \frac{2}{\pi}\ln\left[\frac{1-\cos B\sin D+(1-\cos B)(\cos^2 B-\cos^2 D)^{\frac{1}{2}}}{\sin B(1-\cos B)}\right] - 2\mathscr{D}_1/\mathscr{D}_2[(\cos^2 B/\cos^2 D)-1]^{\frac{1}{2}}, \quad (39a)$$

$$\Pi_{X,\mathrm{G}} = \pi/\mathscr{D}_2[(\cos^2 B/\cos^2 D)-1]^{\frac{1}{2}}. \quad (39b)$$

These functions are plotted against b/l in figure 9. Except for the singular case $l/h = 1$, $\Gamma_{X,G}$ goes to infinity at both $b/l = 0$ and $b/l = 1$; i.e. gravity produces infinite horizontal accelerations at both the bottom and at the lip of the gate. Between these limits, $\Gamma_{X,G}$ has a minimum, whose magnitude is of order unity except for values of l/h near zero or unity. The function $\Pi_{X,G}$ is finite at the bottom, $b/l = 0$, but becomes infinite at the lip of the gate, $b/l = 1$. Due to the singularity at the lip of the gate, the value of $X^{(2)}$ changes discontinuously there, from either a finite or infinite value, to zero.

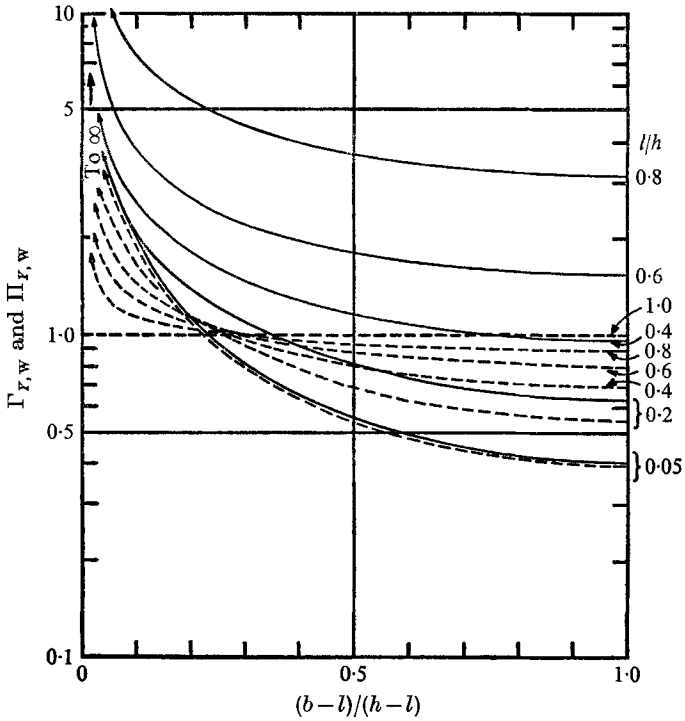

FIGURE 8. The functions Γ_Y and Π_Y for the end wall, as given by (38): ——, $\Pi_{,W}$; – – –, $\Gamma_{Y,W}$.

(*d*) *The bottom* (B): $A \geqslant 0$, $B = 0$. Here $Y_B^{(2)} = 0$, $\Gamma_{Y,B} = 0$, and $\Pi_{Y,B} = 0$. Again the horizontal acceleration on the bottom may be simply deduced from that at the gate. At the gate, $X^{(2)} = W(iB) - i$; while, on the bottom, $X^{(2)} = W(A)$. Thus, the value of $X^{(2)}$ at the bottom is obtained by substituting A in place of iB in (39) and adding i. The results are

$$\Gamma_{X,B} = \frac{2}{\pi} \ln\left[\frac{\cosh A \sin D - 1 + (\cosh A - 1)(\cosh^2 A - \cos^2 D)^{\frac{1}{2}}}{\sinh A(\cosh A - 1)}\right] - 2\mathscr{D}_1/\mathscr{D}_2[(\cosh^2 A/\cos^2 D) - 1]^{\frac{1}{2}}, \quad (40a)$$

$$\Pi_{X,B} = \pi/\mathscr{D}_2[(\cosh^2 A/\cos^2 D) - 1]^{\frac{1}{2}}. \quad (40b)$$

Figure 10 shows these functions. The value of $\Gamma_{X,B}$ becomes infinite as $a/h \to 0$, showing that the horizontal acceleration due to gravity is infinite at the intersection of the bottom and the gate. At $a/h = 0$, $\Pi_{X,B}$ is finite and has zero slope;

hence the horizontal acceleration on the bottom due to pressure differential is nearly constant near the gate. The values of $\Pi_{X,B}$ at $a/h = 0$ agree with the values of $\Pi_{X,G}$ at $b/l = 0$ on figure 9, thereby indicating that the horizontal acceleration on the bottom does not change discontinuously at $a = 0$.

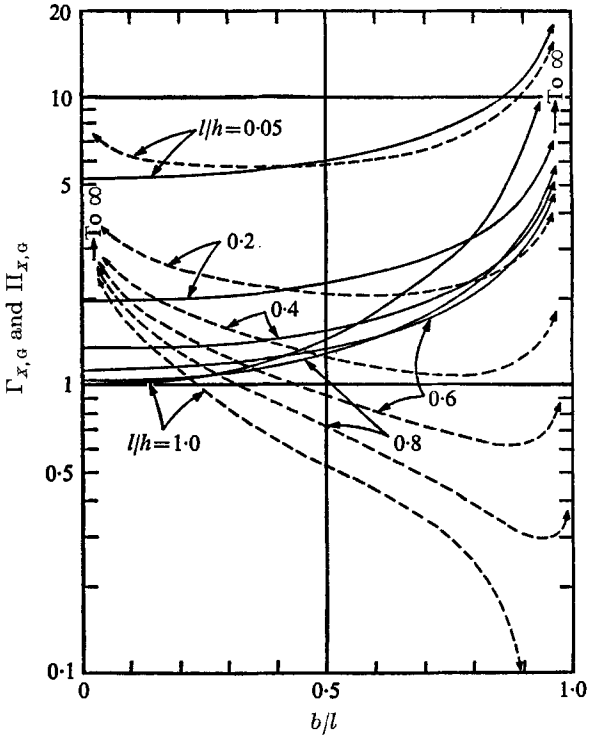

FIGURE 9. The functions Γ_Y and Π_X for the gate, as given by (39): ——, $\Pi_{X,G}$; – – –, $\Gamma_{X,G}$.

(iii) *Conditions far from the end wall and gate*: $A \gg 1$

For $A \gg 1$, the results for the free surface and the bottom have the following limiting forms:

$$\Gamma_{Y,FS} \cong 4\left(\frac{1}{\pi}\sin D - \frac{\mathscr{D}_1}{\mathscr{D}_2}\cos D\right)e^{-A}, \tag{41a}$$

$$\Pi_{Y,FS} \cong \frac{2\pi\cos D}{\mathscr{D}_2}\,e^{-A}, \tag{41b}$$

and

$$\Gamma_{X,B} \cong -\frac{4\mathscr{D}_1\cos D}{\mathscr{D}_2}e^{-A}, \tag{42a}$$

$$\Pi_{X,B} \cong \frac{2\pi\cos D}{\mathscr{D}_2}\,e^{-A}. \tag{42b}$$

On both boundaries, therefore, Γ and Π decay as e^{-A}. On figures 7 and 10, accordingly, which are semi-logarithmic, all the curves approach straight-line asymptotes having the same slope. Equations (41) and (42) may be used as a guide in extending these curves, and are also quite accurate when $A > 2$.

Far from the end wall and gate, one might surmise from the geometry that the flow is one-dimensional, as in the case of a steady-flow discharge from a pressurized reservoir through a gate. But this is not true for the unsteady flow considered here. Indeed, it cannot be true, owing to the inherent differences in the boundary conditions at the free surface and the bottom, as shown in figure 2.

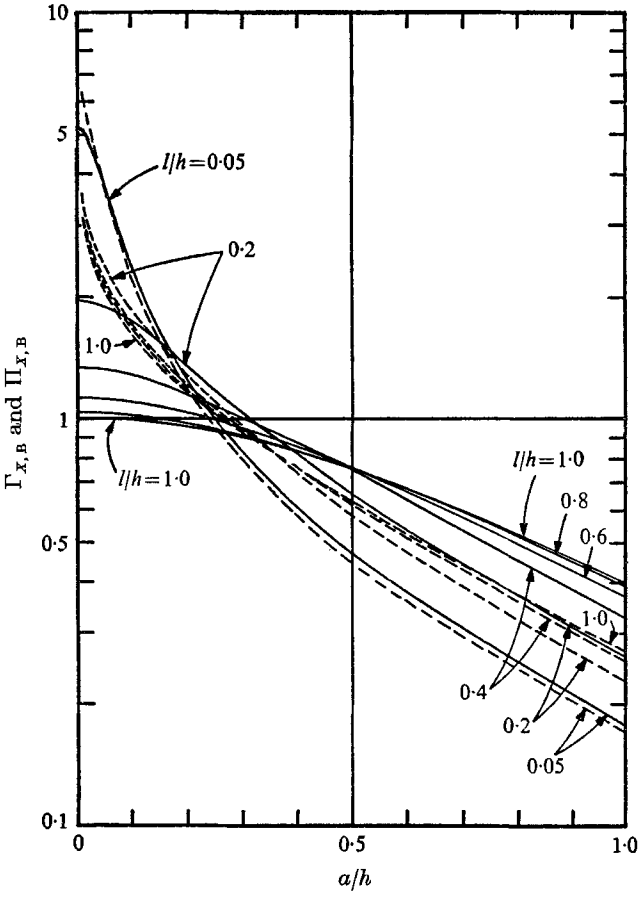

FIGURE 10. The functions Γ_X and Π_X for the bottom, as given by (40): ——, $\Pi_{X,B}$; – – –, $\Gamma_{X,B}$.

(iv) *Rate of discharge through the gate*

The volume flow rate $\dot{Q}$ (per unit width normal to the paper) escaping through the gate may be calculated either as the rate of decrease of the liquid volume contained in the tank, or as the integrated volume flux rate through the gate. Choosing the former method, we may write

$$(\tfrac{1}{2}\pi)^{\frac{3}{2}} g^{-\frac{1}{2}} h^{-\frac{3}{2}} \dot{Q} = -(d/dT)\int_0^\infty (Y_{\mathrm{FS}} - B_{\mathrm{FS}})\, dA,$$

$$= T\left[\int_0^\infty \Gamma_{Y,\mathrm{FS}}\, dA + \frac{\Delta p}{\rho g h}\int_0^\infty \Pi_{Y,\mathrm{FS}}\, dA\right]. \quad (43)$$

Thus $\dot{Q}$ increases linearly with time, and is made up of two additive terms, one representing gravity, the other the pressure differential. The two integrals of (43), which depend upon D, must be found by numerical integration. They are shown in figure 11. For small values of the gate opening ratio, l/h, both curves coincide and are linear with $\ln(l/h)$. The gravity integral remains roughly linear with $\ln(l/h)$ over the entire range, whereas the pressure integral goes to infinity as $l/h \to 1$.

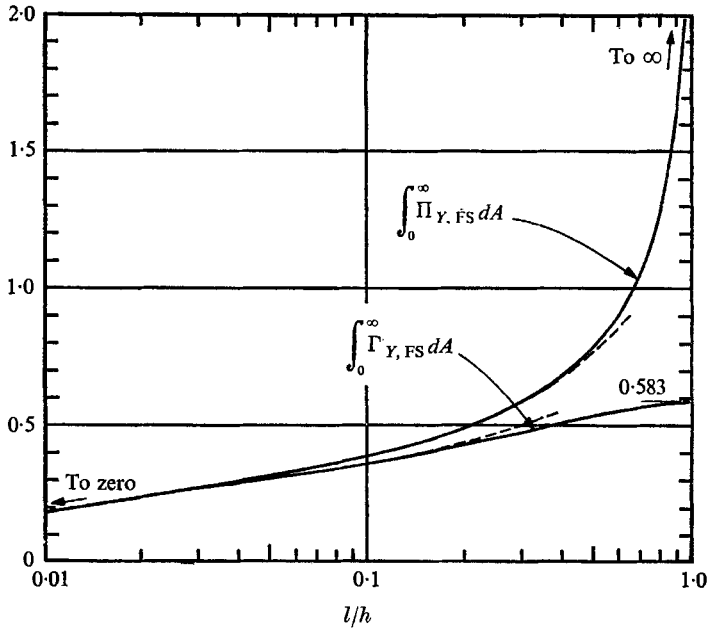

FIGURE 11. The flow rate integrals of (43): ——, exact solutions; – – –, expansion solutions, (50), for $l/h \ll 1$.

(v) *The limit of small gate opening*, $D \to 0$

It is convenient to develop the limiting forms of the solution functions for very small gate openings, $D \ll 1$. This is not only because certain of the Γ's and Π's go to zero, but also because the formulas take simpler explicit forms as $D \to 0$. In this limit, the sources and sinks cancel, and only the doublet survives in the ζ_2-plane. The complex potential is approximated by

$$W(Z) = X^{(2)} - iY^{(2)} \cong -2\mu/\sinh Z. \tag{44}$$

(*a*) *The functions* $\mathscr{D}_1(D)$ *and* $\mathscr{D}_2(D)$. Expansions of the terms in (29) and (31) lead to the results:

$$\mathscr{D}_1 = -\tfrac{1}{2}\pi - (2/\pi)D\ln\tfrac{1}{2}D + D + \ldots, \tag{45a}$$

$$\mathscr{D}_2 = -2\ln D + 4\ln 2 + \tfrac{3}{4}D^2\ln D + \ldots. \tag{45b}$$

These show that, as $D \to 0$, $\mathscr{D}_1 \to -\tfrac{1}{2}\pi$ and $\mathscr{D}_2 \to \infty$. Therefore the doublet strength μ approaches zero unless $\Delta P \to \infty$. The dashed curves on figure 6 represent the approximations of (45*a*) and (45*b*). They are very close to the exact results up to $l/h = 0{\cdot}3$.

(*b*) *The functions* Γ *and* Π. We give here the limiting forms for $D \ll 1$:

$$\Gamma_{Y,\mathrm{FS}} \cong -\frac{\pi}{2\ln D\cosh A}\left[\left(1-\frac{2\ln 2}{\ln D}\right)^{-1}+\left(\frac{4}{\pi^2}\ln 2-\frac{2}{\pi}\right)D\right], \tag{46a}$$

$$\Pi_{Y,\mathrm{FS}} = -\frac{\pi}{2\ln D\cosh A}\left(1-\frac{2\ln 2}{\ln D}\right)^{-1}+O(D), \tag{46b}$$

$$\Gamma_{Y,\mathrm{W}} = \Pi_{Y,\mathrm{W}} = -\frac{\pi}{2\ln D\sin B}\left(1-\frac{2\ln 2}{\ln D}\right)^{-1}+O(D), \tag{47}$$

$$\Gamma_{Y,\mathrm{B}} = \Pi_{Y,\mathrm{B}} = -\frac{\pi}{2\ln D\sinh A}\left(1-\frac{2\ln 2}{\ln D}\right)^{-1}+O(D). \tag{48}$$

Note that the values of Γ and Π shown above not only go to zero as $D\to 0$, but also become identical for $D \ll 1$. For the acceleration at the gate, both B and D must be assumed $\ll 1$ in this case. The limiting forms are

$$\Gamma_{X,\mathrm{G}} \cong -\pi/2(D^2-B^2)^{\frac{1}{2}}\ln D-(6/\pi)\ln B, \tag{49a}$$

$$\Pi_{X,\mathrm{G}} = -\pi/2(D^2-B^2)^{\frac{1}{2}}\ln D+O(1/\ln D). \tag{49b}$$

It is clear that $\Gamma_{X,\mathrm{G}}$ and $\Pi_{X,\mathrm{G}}\to\infty$ as $D\to 0$. Although the dominant term in the two expansions is the same, the difference $(\Gamma-\Pi)$ is positive and goes to infinity as $B\to 0$.

(*c*) *Discharge through the gate.* The limiting forms of the flow integrals of (43) are

$$\int_0^\infty \Gamma_{Y,\mathrm{FS}}\,dA = -\frac{\pi^2}{4\ln D}\left[\left(1-\frac{2\ln 2}{\ln D}\right)^{-1}+\left(\frac{4}{\pi^2}\ln 2-\frac{2}{\pi}\right)D\right]+\ldots, \tag{50a}$$

$$\int_0^\infty \Pi_{Y,\mathrm{FS}}\,dA = -\frac{\pi^2}{4\ln D}\left(1-\frac{2\ln 2}{\ln D}\right)^{-1}+O(D^2). \tag{50b}$$

These are graphed by dashed lines in figure 11, where it is is seen that close agreement with the exact solution is obtained up to $l/h \cong 0{\cdot}4$.

(vi) *The limit of large gate opening,* $D\to\frac{1}{2}\pi$ (*or* $l/h\to 1$)

Here it is convenient to define the small parameter $\delta \equiv (\frac{1}{2}\pi)-D$. Expansion of equations (29) and (31) in δ then yields

$$\mathscr{D}_1 = -\tfrac{1}{2}\delta^2+\ldots, \tag{51a}$$

$$\mathscr{D}_2 = \pi\delta(1+\tfrac{1}{12}\delta^2)+\ldots. \tag{51b}$$

These are shown by dot–dash curves on figure 6, and agree with the exact values quite well for $l/h > 0{\cdot}4$.

The limiting forms of the acceleration functions at the free surface are

$$\Gamma_{Y,\mathrm{FS}} = \frac{2}{\pi}\tan^{-1}\left(\frac{1}{\sinh A}\right)+\frac{\delta^2}{\pi}\left(1-\frac{1}{\sinh A\cosh^2 A}\right)+\ldots, \tag{52a}$$

$$\Pi_{Y,\mathrm{FS}} = \frac{1}{\sinh A}\left[1-\frac{\delta^2}{2}\left(\frac{1}{6}+\frac{1}{\sinh^2 A}\right)\right]+\ldots. \tag{52b}$$

As expected, the first term of the gravitational contribution, equation (52*a*), is identical with the result given by Stoker (1957) for the solution of the dam-

breaking problem. The solution for the pressure-differential contribution, (52*b*), is meaningful only until such time as the free surface in the tank joins the free surface at the gate. Beyond that, the pressure differential Δp vanishes, and the present solution cannot be continued because the boundary conditions are different in form.

Some additional remarks may be made here concerning the case $D = \frac{1}{2}\pi$, i.e. the dam-breaking problem, for which there is no wall. This limit of the more general solution given in this paper is singular, in the sense that the boundary condition $X^{(2)} = 0$ at $A = 0$, $B = \frac{1}{2}\pi$ changes discontinuously as $D \to \frac{1}{2}\pi$. The singular nature of the case $D = \frac{1}{2}\pi$ (or $l/h = 1$) has already been mentioned in connexion with the curves of figures 7–9. In figure 7, the curves for $l/h = 1$ show different behaviour from all the others as $a/h \to 0$. In figure 8, $\Pi_{Y,W} = \infty$ for $l/h = 1$. In figure 9, as $b/l \to 1$, $\Gamma_{X,G}$ goes to $+\infty$ for all values of l/h except $l/h = 1$, for which it goes to zero.

(vii) *Are Δp and ρgh equivalent?*

While the gravity term ρgh may be thought of as a driving pressure difference, it is not equivalent to an equal pressure differential Δp. The reason is that gravity acts uniformly throughout the bulk of the fluid, whereas Δp is established uniformly only at the two free surfaces. That their effects are different is evident from figures 7, 8 and 10, where the curves for Γ and Π differ substantially from each other if $l/h > 0{\cdot}05$; and from figure 9, where the curves are inherently different in form.

In the limit of $l/h \to 0$, however, with the exception of the gate, the curves for Γ and Π approach each other in figures 7, 8 and 10. This coincidence of Γ and Π is confirmed by (46), (47) and (48). If the gate opening is very small, therefore, a pressure differential alone, of magnitude $\Delta p = \rho gh$, produces the same motion as gravity alone, except in the vicinity of the gate. Conversely, a negative pressure differential, of magnitude $\Delta p = -\rho gh$, exactly balances the effect of gravity far from the gate if $l/h \ll 1$.

Near the gate, as shown by figure 9 and (49), Γ and Π are essentially different, even as $l/h \to 0$. At this limit, the values of $X^{(2)}$ and $Y^{(2)}$ are so small as to be negligible throughout most of the fluid; the situation then approximates hydrostatic equilibrium, and thus Δp and ρgh produce virtually equivalent effects. Near the gate, however, dynamic effects persist for $l/h \to 0$, so that Δp and ρgh are not equivalent.

(viii) *Contours of constant $Y^{(2)}$*

Five different types of solution exist, depending upon the magnitude of μ. Since $\mathscr{D}_2 > 0$ and $\mathscr{D}_1 < 0$, (32) shows that $\mu > 0$ when ΔP is either positive or only mildly negative. For sufficiently large negative values of ΔP, μ takes on negative values.

(*a*) *Positive values of μ.* Figure 2, and the corresponding mappings of figures 4 and 5, show the contours of constant $Y^{(2)}$ when μ is positive but not large. The value of $-Y^{(2)}$ on the free surface is everywhere less than unity (i.e. the acceleration is less than that of gravity), but reaches and exceeds unity on the end wall.

(*b*) Figure 12(*a*) corresponds to a case with a very large positive value of μ. The singular curves of $Y^{(2)}$ are different in form from those of figure 2. Over part of the free surface, $-Y^{(2)} > 1$, and the vertical acceleration exceeds that of gravity over the entire end wall.

(*c*) *Negative values of* μ. Figures 12(*b*), (*c*) and (*d*) show the $Y^{(2)}$ contours for negative values of ΔP (and also of μ) that are increasingly large. The three cases illustrate the different types of singular curves that occur.

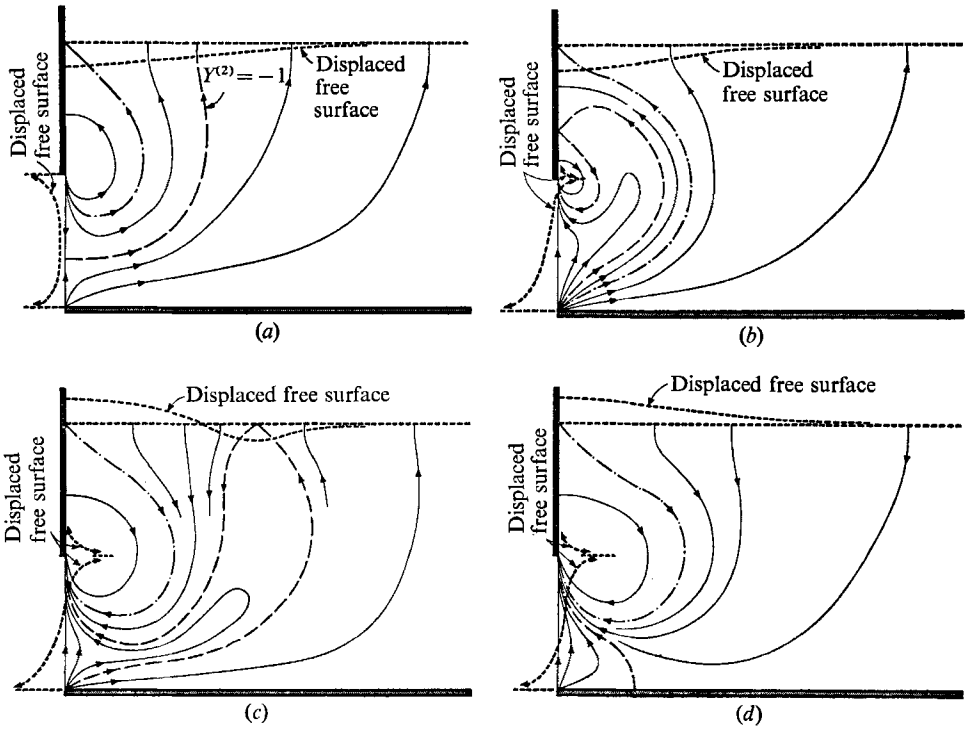

FIGURE 12.† Schematic sketches showing contours of constant $Y^{(2)}$ and displaced shapes of free surfaces. See also figure 2. (*a*) $\mu > 0$, large $|\mu|$. The free surface shapes pertain to any positive value of μ. The $Y^{(2)}$ contours pertain to large positive values of μ, while figure 2 shows the $Y^{(2)}$ contours for small values of μ. (*b*, *c*, *d*) Successively larger negative values of μ: (*b*) $\mu < 0$, small $|\mu|$; (*c*) $\mu < 0$, medium $|\mu|$; (*d*) $\mu < 0$, large $|\mu|$.

† The ranges of applicability are as follows:

figure 2 $$\frac{\mathscr{D}_2}{\pi}\left(1-\frac{2D}{\pi}\right)+\frac{2\mathscr{D}_1}{\pi} > \frac{\Delta p}{\rho g h} > \frac{2\mathscr{D}_1}{\pi};$$

figure 12(*a*) $$\frac{\Delta p}{\rho g h} > \frac{2\mathscr{D}_1}{\pi}+\frac{\mathscr{D}_2}{\pi}\left(1-\frac{2D}{\pi}\right);$$

(*b*) $$\frac{2D\mathscr{D}_2}{\pi^2}-\frac{2\mathscr{D}_1}{\pi} > -\frac{\Delta p}{\rho g h} > -\frac{2\mathscr{D}_1}{\pi};$$

(*c*) $$\frac{2\mathscr{D}_2 \tan D}{\pi^2}-\frac{2\mathscr{D}_1}{\pi} > -\frac{\Delta p}{\rho g h} > \frac{2D\mathscr{D}_2}{\pi^2}-\frac{2\mathscr{D}_1}{\pi};$$

(*d*) $$-\frac{\Delta p}{\rho g h} > \frac{2\mathscr{D}_2 \tan D}{\pi^2}-\frac{2\mathscr{D}_1}{\pi}.$$

(ix) *Shapes of free surfaces*

Figure 12 also shows schematically the different kinds of free-surface displacements that can occur, as determined by $Y_{FS}^{(2)}$ for the liquid surface in the tank, and by $X_G^{(2)}$ for the surface at the gate.

(*a*) *Positive values of* μ. As long as μ is positive, no matter how large or how small, the free surfaces are displaced as in figure 12(*a*). Within the tank, the free surface everywhere accelerates downward, increasingly so near the end wall; somewhat surprisingly, the slope at the end wall is zero (one might have guessed otherwise). At the gate, $X_G^{(2)} = -\infty$ at both $b = 0$ and $b = l$. Accordingly, the jet always squirts out horizontally. There is always a minimum in $-X_G^{(2)}$ and thus the displaced free surface appears as in figure 12(*a*).

(*b*) *Negative values of* μ. Figures 12(*b*), (*c*) and (*d*) illustrates schematically the successive varieties of free-surface displacement that occur as μ takes on larger and larger negative values. Two features are particularly interesting. The first is that, at $a = 0$, $b = 0$, $X^{(2)} = -\infty$ no matter how large a negative value of ΔP is applied. Thus, as seen in figure 12(*d*), a small amount of liquid will always issue from the tank near the bottom. This is of some practical importance when a pressure difference is used as a means of averting the escape of dangerous liquids stored in a tank. The second is that, just under the lip of the gate ($a = 0$, $b = l^-$), $X^{(2)} = +\infty$; while just above the lip of the gate ($a = 0$, $b = l^+$), $Y^{(2)} = +\infty$. Thus, a double free surface is formed, with its leading edge having a cusp. The latter would in practice be rounded by surface tension.

(x) *Remarks on a more general geometry*

The procedures used for solving the problem of this paper point to the method of solution for a more general problem: that in which the gate is not in the bottom of the end wall, but somewhere between top and bottom. An additional geometric parameter now appears. By means of combinations of analytical continuations and of Schwartz–Christoffel transformations, the value of $Y^{(2)}$ can be prescribed on the horizontal axis of a half-plane, as in figure 5. There will now be four doublets present, corresponding to the singularities at both the upper and lower sides of the gate, and to their corresponding reflected singularities. That two different doublet strengths, μ_a and μ_b, must now be determined causes no inherent difficulty, since the pressure boundary condition of (21) can be applied twice: one going through the doublet μ_a, the second going through the doublet μ_b.

This work was supported in part by the National Institute of Health under contract PH3 67 1114.

REFERENCES

Kolff, W. J., Moulopoulos, S. D. & Topaz, S. R. 1962 Diastolic balloon pumping (with carbon dioxide) in the aorta, a mechanical assistance to the failing circulation. *Am. Heart J.* **63**, 669–675.

McMahon, T. A. 1969 The dynamics and fluid mechanics of the intra-aortic balloon heart assist device. Ph.D. Thesis, Department of Aeronautics and Astronautics, M.I.T.

Pohle, F. V. 1952 Motions of water due to breaking of a dam, and related problems. *U.S. National Bureau of Standards, Gravity Waves, N.B.S. Circular* 521.

Stoker, J. J. 1957 *Water Waves.* New York: Interscience.